Non-coding RNA Research 11 (2025) 262–272

Contents lists available at ScienceDirect

Non-coding RNA Research

journal homepage: www.keaipublishing.com/en/journals/non-coding-rna-research

Original Research Article

Long non-coding RNA AK023617 orchestrates atherosclerosis by regulating the circadian rhythm of immunity-related GTPase family M protein in macrophages

Rongzhe Lu [a,b,1], Hengxuan Cai [a,b,1], Yige Liu [a,b], Guanpeng Ma [a,b], Jiaxin Wang [a,b], Miao Yan [a,b], Zhenming Zhang [a,b], Bo Yu [a,b,*], Zhaoying Li [a,b,*], Shaohong Fang [a,b,*]

[a] The Key Laboratory of Myocardial Ischemia, Harbin Medical University, Ministry of Education, Harbin, Heilongjiang Province, China
[b] Department of Cardiology, The 2nd Affiliated Hospital of Harbin Medical University, Harbin, Heilongjiang Province, China

ARTICLE INFO

Keywords:
Circadian rhythm
Long non-coding RNA
Macrophage
Necroptosis
Atherosclerotic plaque stability

ABSTRACT

Acute coronary events show a diurnal rhythm, and atherosclerotic plaque vulnerability, as a histomorphological characteristic of major adverse cardiovascular events, is a key target for intervention. Although oscillating microRNAs reduce plaque stability by facilitating macrophage apoptosis in lesions, whether rhythmic long non-coding RNA (lncRNA) can regulate diurnal oscillations in plaque stability and the potential underlying mechanism remain unclear. In this study, we examined whether rhythmic lncRNAs are involved in the pathogenesis and progression of atherosclerosis and detected a novel circadian lncRNA-AK023617, which is positively correlated with the peak occurrence of major adverse cardiovascular events. Transfection of short interfering RNA specific to lnc-AK023617 into THP-1 cells dampened the oscillation of immunity-related GTPase family M protein 1 (Irgm1), which is negatively related to plaque stability. In ApoE$^{-/-}$ mice fed a high-fat diet for 12 weeks, diurnal variations in lncAK023617 were consistent with the proportions of necroptotic cells in atherosclerotic plaques. In addition, reduced expression of lncAK023617 inhibited P-RIP3 and P-MLKL in THP-1 cells. Mechanistically, lncAK023617 interacted with the core molecular clock Bmal1 and promoted nuclear translocation of Bmal1, which could directly bind to the E-BOX elements in the *Irgm1* promoter. Thus, oscillating lncAK023617 in macrophages can affect plaque stability by regulating necroptosis, which regulates circadian expression of the target gene *Irgm1* by increasing the transcriptional activity of Bmal1, ultimately determining the diurnal oscillations in plaque stability. Therefore, lncAK023617 may serve as a specific target to ameliorate atherosclerotic plaque vulnerability.

1. Introduction

In mammals, circadian rhythms are regulated by a central clock and peripheral clocks. Light information, the main clock input signal, is processed via the retinohypothalamic tract and transmitted to the suprachiasmatic nucleus, which is the master clock [1]. The peripheral molecular clocks consist of core clock components such as aryl hydrocarbon receptor nuclear translocator-like protein 1 (also known as BMAL1) and circadian locomotor output cycles protein kaput (CLOCK) that form complex auto-regulatory transcription-translation feedback loops [2]. BMAL1 forms a heterodimeric partnership with CLOCK and binds to E-box sites across the genome, inducing rhythmic expression in clock-controlled genes through a transcriptional mechanism [3].

A growing body of epidemiological data shows the occurrence of daily oscillations in major adverse cardiovascular events such as stroke [4], myocardial infarction [5], severe ventricular arrhythmia [6], and sudden cardiac death [7]. Atherosclerosis (AS) is the primary cause of most cardiovascular diseases, and macrophages participate in the entire process of atheromatous plaque formation [8]. The CCL2-CCR2 axis, which is regulated by the clock protein Bmal1 and REV-ERBα, modulates rhythmic pro-inflammatory monocyte recruitment and adhesion to atherosclerotic lesions [9].

Vulnerable plaques have large necrotic cores, accompanied by

* Corresponding author;The Key Laboratory of Myocardial Ischemia, Harbin Medical University, Ministry of Education, Harbin, Heilongjiang Province, China
E-mail addresses: lizhaoying1990@hrbmu.edu.cn (B. Yu), dryu_hmu@163.com (Z. Li), fangshaohong@hrbmu.edu.cn (S. Fang).
[1] These authors contributed equally to this work: Rongzhe Lu, Hengxuan Cai.

https://doi.org/10.1016/j.ncrna.2024.12.008
Received 20 September 2024; Received in revised form 8 November 2024; Accepted 16 December 2024
Available online 22 December 2024

Abbreviations

AMI	acute myocardial infarction
AS	atherosclerosis
lncRNA	long non-coding RNA
ApoE	apolipoprotein E
ox-LDL	oxidized low density lipoprotein

substantial macrophage infiltration [10]. Macrophage death is the major cause of the formation of necrotic cores [11]. Kung et al. discovered a caspase-independent programmed form of cell death, termed necroptosis, in cardiovascular disease [12]. In AS, triggers of necroptosis include TNF under caspase inhibition, oxidized low-density lipoprotein (ox-LDL), and IFNγ [13]. Necroptosis is also negatively regulated by caspase-8, which is mediated by the kinase activities of receptor-interacting serine/threonine-protein 1 (RIP1; or receptor-interacting serine/threonine-protein kinase 1, RIPK1). Cascade phosphorylation of receptor-interacting serine/threonine-protein kinase (RIPK3) and mixed lineage kinase domain-like protein (MLKL) contributes to permeabilization of the plasma membranes, release of damage-associated molecular patterns, and, eventually, necroptosis [14]. During AS development, the accumulation of ox-LDL in the subendothelial space can trigger necroptosis in macrophages [15]. Necroptosis of macrophages essentially contributes to the formation of necrotic core and plaque vulnerability and accelerates the development of AS [16]. Circadian expression of microRNA-21 in macrophages can promote AS progression and increase plaque vulnerability by regulating diurnal oscillations in apoptosis [17]; however, whether necroptosis in plaques shows a diurnal rhythm remains unclear.

Long non-coding RNAs (lncRNAs) have emerged as major regulators of various biological processes and are characterized by tissue- and cell-specific expression and diverse regulatory modes [18,19]. LncRNAs have been implicated in circadian clock regulation; most oscillating lncRNAs discovered to date are involved in cancer and steatohepatitis [20,21]. However, the precise mechanism underlying the regulatory role of rhythmic lncRNAs in cardiovascular diseases remains unclear. A previous study demonstrated that lncNEAT1 provided cardiovascular protection by sustaining circadian oscillators in vascular smooth muscle cells [22]. Therefore, our objective was to comprehensively investigate and determine whether rhythmic lncRNAs present in other cells involved in the pathogenesis and progression of AS could regulate disease severity.

In the present study, we demonstrated that the circadian expression of lncRNA-AK023617 promotes the circadian oscillations of necroptosis in ox-LDL-stimulated macrophages by regulating the rhythmic expression of the target gene IRGM via the nuclear translocation of Bmal1. This mechanism enables the molecular clock to modulate necroptosis, a form of cell death, thereby offering a potential therapeutic approach for treating AS by disrupting the rhythmic oscillations in plaque vulnerability.

2. Material and methods

2.1. Patients

In total, 3502 patients who underwent emergency percutaneous coronary intervention (PCI) surgery at the Chest Pain Center of the Second Affiliated Hospital of Harbin Medical University (Harbin, China) in 2019 were included. The number of patients was recorded every 4 h starting from sunrise time (5:00 a.m.; Zeitgeber [ZT] 0). The main exclusion criteria were angina pectoris, myocarditis, heart failure, aortic dissection, acute and chronic infections and infectious diseases, hepatic and renal insufficiency, and severe progressive diseases. Finally, 59 patients with acute myocardial infarction (AMI) were selected for peripheral white blood cell extraction. We analyzed optical coherence tomography (OCT) images and obtained the serum of 13 versus 7 AMI patients at ZT4 and ZT16 (Table S1). Triglyceride (TG), total cholesterol (TC), low-density lipoprotein cholesterol (LDL-C) and high-density lipoprotein cholesterol (HDL-C) were tested by a microplate reader following the manufacturers' instructions (Tecan, Männedorf, Switzerland).

Blood samples of the patients were centrifuged at 4 °C, 3000 rpm for 10 min, and the lower whole-blood fraction was supplemented with PBS and lymphoid separation solution (TBD, Tianjin, China). Then, leukocytes of patients were harvested according to the manufacturer's instructions. The leukocytes were collected by TRIzol reagent (Thermo Fisher, Waltham, MA, USA) and stored at −80 °C for detecting the expression of lncAK023617 and IRGM through quantitative reverse transcription (RT-q) PCR.

2.2. Animals

Male ApoE$^{-/-}$ mice with a C57BL/6 background (8 weeks old) were obtained from Charles River Animal Center (Beijing, China). All mice were housed in a temperature-controlled environment (24–25 °C, humidity: 55 %) under a 12 h/12 h light/dark cycle (lights on at 7 a.m. and off at 7 p.m.), with free access to food and water. The mice were maintained on the normal diet (ND) or the high-fat diet (HFD) consisting of 78.85 % base feed, 21 % fat, and 0.15 % cholesterol for 12 weeks. After 12 weeks of HFD feeding, Peripheral blood, aortas and hearts were harvested every 4 h starting from 7 a.m. (ZT0) and fixed with optimal cutting temperature compound (Thermo Fisher, USA).

To evaluate the effects of AK023617 inhibition on circadian oscillations in stability of advanced atherosclerotic plaques, male ApoE$^{-/-}$ mice were fed a high-fat diet (HFD) for 12 weeks and then randomly assigned to groups. The mice were given tail vein injections of 100 μL of vehicle containing 1.0×10^{12} AAV2/9 vector particles (negative control shRNA [sh-NC] or lncRNA- AK023617 shRNA [sh-AK023617], Hanbio Biotechnology, Co., Ltd., Wuhan, China) or 100 μL of saline as a control at Zeitgeber Time 16 (ZT16). After 15 days, the mice were sacrificed, and the aortas and hearts were collected for expression and histological analyses.

2.3. Cell culture

THP-1 cells were purchased from the China Center for Type Culture Collection. The cells were cultured in RPMI 1640 medium (88,365; Gibco, Carlsbad, CA, USA) supplemented with 10 % fetal bovine serum. After overnight incubation, the cells were incubated for 2 h with 50 % horse serum to achieve synchronization., then the medium was replaced with a serum-free medium. After synchronization, the THP-1 cells were harvested for RNA isolation every 4 h over a 24 h period. Before harvest, the cells were transfected with negative control (si-NC) or si-lncAK023617 (20 nM) (R11062.2; Ribo Bio, China) by Lipo3000 (L3000008, Invitrogen, USA) for 4 h. Subsequently, they were stimulated with ox-LDL (50 μg/mL) (YB-002; Yiyuan Biotech, China) for 24 h.

2.4. LncRNA-mRNA co-expression network

The lncRNA-mRNA co-expression network was constructed between the differentially expressed lncRNAs and mRNAs and subsequently imported into Cytoscape software. We used Pearson's correlations, equal to or greater than 0.99, to calculate statistically significant associations.

2.5. RNA pull-down

LncAK023617 sense or antisense RNA was prepared using *in vitro* transcription of appropriately linearized plasmid templates (Cat. AM1344, Invitrogen, USA). Then, biotinylated RNAs were synthesized

and used for RNA pull-down assay according to the manufacturer's instructions (Cat. 20,164, Thermo Fisher, USA). RNA-associated proteins were separated by SDS-PAGE (polyacrylamide gel electrophoresis). Then, we performed silver staining using a fast silver stain kit (Beyotime, Shanghai, China), western blotting (WB), and subjected to LC-MS analysis.

2.6. RNA immunoprecipitation

RNA immunoprecipitation (RIP) experiments were performed using a Magna RIP™ RNA-Binding Protein Immunoprecipitation Kit (Cat. 17–701, Millipore, Billerica, MA, USA). Cell lysates were isolated from THP-1 which was stimulated with oxidized low-density lipoprotein (ox-LDL; 50 μg/mL) and treated with RNase inhibitor and protease inhibitor, followed by incubation with human *anti*-Bmal1 antibody (14,020, Cell Signaling Technology [CST], USA) or normal rabbit IgG (2729, CST, USA) antibody at 4 °C overnight. Antibody/protein/RNA complexes were immunoprecipitated with protein A/G beads. RNA associated with Bmal1 was extracted with TRIzol and analyzed by RT-qPCR.

2.7. Chromatin immunoprecipitation assay

We used an EZ-Magna ChIP Kit (Millipore, Billerica, USA) for chromatin immunoprecipitation (CHIP) assays according to the manufacturer's instructions. Briefly, we used 4 % formaldehyde to generate DNA-protein crosslinks in THP-1 cells. The cell lysates were sonicated to generate chromatin fragments of approximately 70–100 bp followed by immunoprecipitation with Bmal1 antibody (14,020, CST, USA) or the control antibody IgG (Millipore, Billerica, USA). Finally, we used qPCR to quantify the precipitated chromatin DNA.

2.8. Quantitative reverse transcription (RT-q) PCR and WB

The experimental methods for RT-qPCR and WB have been described in our previous publication [23]. RNA was extracted from THP-1 cells using a cytoplasmic/nuclear RNA purification kit (NGB-21000, Norgen Biotek, USA). The following primers were used for qPCR were listed in the file of Table S2.

The following antibodies were used for WB: *anti*-P-RIP3 (91,702, CST, USA), anti-RIP3 (95,702, CST, USA), *anti*-P-MLKL (AP0949, ABclonal, China), *anti*-MLKL (A5579, ABclonal, China), *anti*-Bmal1 (14,020, CST, USA), *anti*-GAPDH (ta-08, ZSBG-Bio, China), and anti-Histone 3 (14269s, CST, USA).

2.9. Flow cytometry

THP-1 cells were transfected with si-NC, si-IRGM or si-lncAK023617 using Lipo3000 (L3000008, Invitrogen, USA) for 6 h. Subsequently, they were stimulated with ox-LDL (50 μg/mL) for 24 h. Annexin V-FITC & PI Apoptosis Detection Kit (556,570, BD Biosciences, USA) and FACSCantoII™ System (BD Biosciences) were used for detecting necroptosis of THP-1 cells. The data were analyzed using FlowJo software (Tree Star).

2.10. Statistical analysis

The data are expressed as the mean ± SD and were evaluated using GraphPad Prism version 9.0. Means were compared using a one-way ANOVA analysis for multiple groups and unpaired Student's *t*-test for two groups. Statistical significance was set at $P < 0.05$. Cosinor analysis was used to obtain circadian rhythm parameters, such as mesor, amplitude, and acrophase. The zero-amplitude test showed that genes with $P < 0.05$ were considered to have a circadian rhythm.

3. Results

3.1. Circadian lncRNA-AK023617 is closely associated with circadian oscillations in plaque stability in patients with acute myocardial infarction in heilongjiang province

First, we analyzed the population statistics of patients who underwent emergency percutaneous coronary intervention in our hospital in 2019 at different zeitgeber times (ZT). The results showed that the peak period of the occurrence of major adverse cardiovascular events was from 9 p.m. to 1 a.m. (ZT16) (Fig. 1A). We identified alterations in the circadian genes of macrophages, the main causative cells of AS, by analyzing RNA-sequencing data from public databases (GSE157878). We found high-amplitude circadian non-coding RNAs in murine bone marrow-derived macrophages (Fig. 1B). Among the group of oscillating non-coding RNAs, NONMMUT031096 exhibited the highest amplitude expression, which was highly homologous to human AK023617 (Fig. 1B and Fig. S1). Notably, AK023617 was predominantly expressed in macrophages among the various cell types associated with atherosclerotic plaques (Fig. S2). LncRNA–AK023617 showed a diurnal expression pattern in the peripheral blood of patients with (AMI) with a peak at ZT16 and trough at ZT4 (Fig. 1C). OCT can reveal the detailed morphologic characteristics of high-risk plaques and has become an essential diagnostic modality for myocardial infarction [24,25]. Thin-cap fibroatheroma, as an important parameter in OCT, including the thinnest fibrous cap thickness, maximum lipid arc, and minimal lumen area, is used to assess the high-risk lesions [25]. According to OCT image analysis, the maximum lipid arc was higher at ZT16 than at ZT4 in patients with AMI, but the mini fibrous cap thickness and minimal lumen area showed no significant changes at different ZTs (Fig. 1D–F). Lipid risk factors, such as cholesterol, triglycerides, and LDL levels in the plasma of patients with AMI were higher at ZT16 than at ZT4 (Fig. 1G–I). In contrast, the HDL level was lower (Fig. 1J). Together, these data indicate that a cycling lncRNA-AK023617 is involved in circadian oscillations in plaque stability.

3.2. Circadian rhythm of lncRNA-AK023617 is consistent with diurnal variations of necroptosis in atherosclerotic lesions

Because lncRNA-AK023617 was diurnally rhythmic, we examined the circadian time variation of this lncRNA in atherosclerotic plaques. The results shown in Fig. 1 suggest that AK023617 is closely related to plaque stability. Next, we investigated the role of murine AK023617 (NONMMUT031096) in plaque stability in atherosclerotic lesions. Murine AK023617 expression levels in lesions from $ApoE^{-/-}$ mice were measured at six different circadian points after 12 weeks of HFD consumption, revealing a trough at ZT4 and peak at ZT16 (Fig. 2A). Furthermore, the higher proportion of the necrotic core, thinner collagen fibrous caps, and more concentrated cholesterol crystals occurred at ZT16 than at ZT4 (Fig. 2B–E). This result was consistent with the rhythmic oscillations in AK023617, suggesting that AK023617 diurnal rhythms regulate diurnal oscillations in the plaque necrotic core, which was a characteristic of vulnerable plaques. Kyoto Encyclopedia of Genes and Genomes (KEGG) pathway analysis of differentially oscillating non-coding RNAs indicated that murine bone marrow-derived macrophages were associated with the TNF signaling pathway and necroptosis (Fig. S3). Necroptosis increases atherosclerotic plaque progression by promoting necrotic core formation [14]. The diurnal variations in AK023617 at ZT4 and ZT16 were highly related to necroptosis in advanced AS (Fig. 2F–H). These results indicate that necroptosis and necrotic core formation are diurnally regulated in advanced AS.

3.3. LncRNA-AK023617 inhibition decreased AS progression at ZT16 in $ApoE^{-/-}$ mice in vivo

Given the potential role of AK023617 in circadian oscillations in

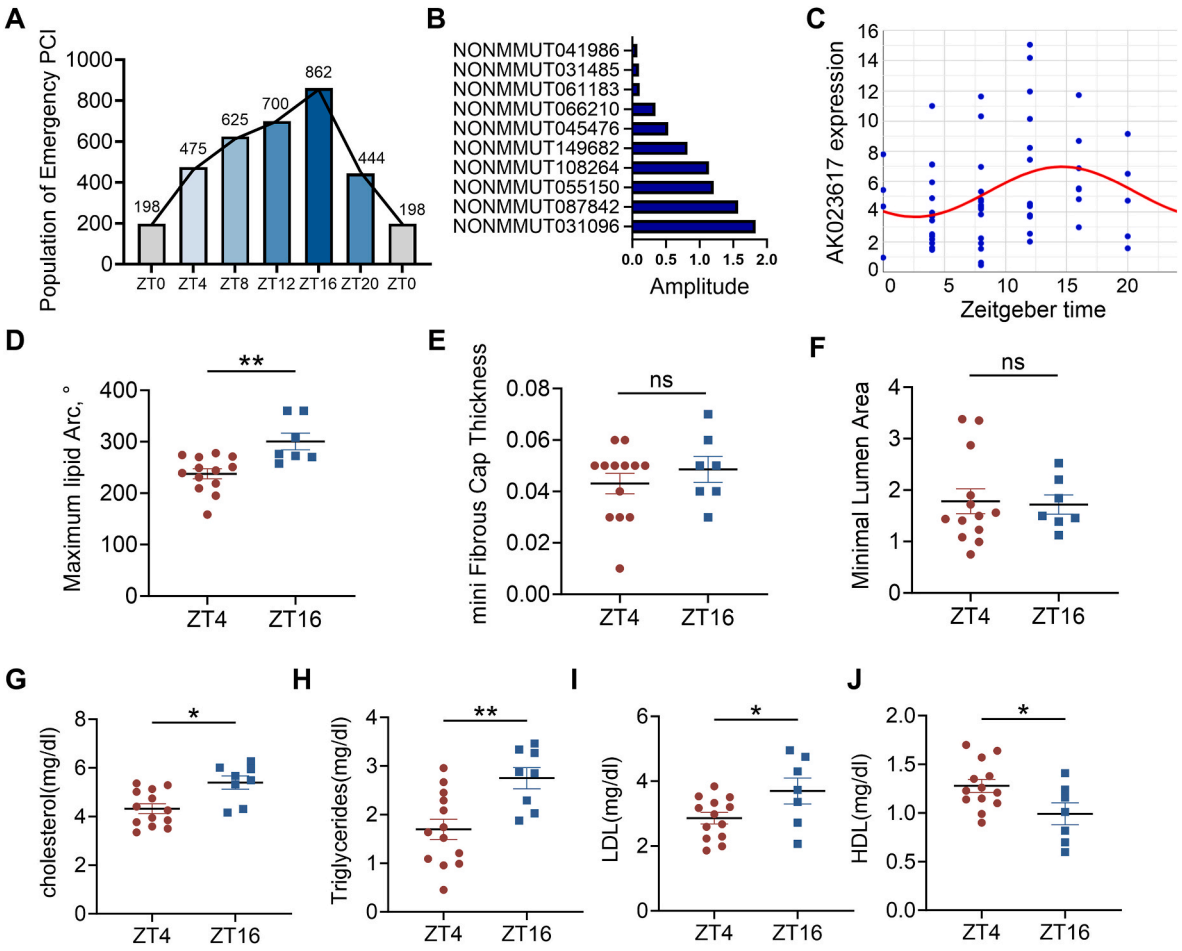

Fig. 1. Oscillating lncRNA-AK023617 is associated with the diurnal occurrence of acute adverse events. A Population statistics of patients undergoing emergency percutaneous coronary intervention at various time points during the year. **B** Top 10 high-amplitude circadian noncoding RNAs in murine bone marrow-derived macrophages. **C** Peripheral blood leukocytes of patients with acute myocardial infarction (AMI) were isolated at 4 h intervals, and lncAK023617 expression was measured using RT-qPCR. The rhythmicity of lncAK023617 was analyzed; mesor = 5.31, amplitude = 1.66, acrophase = 14.60, $P < 0.05$, n = 56. **D–F** Maximum lipid arc, mini–fibrous cap thickness, and minimal lumen area in optical coherence tomography (OCT) analysis in patients with AMI were compared at ZT4 and ZT16. **G–J** Serum cholesterol, triglycerides, low-density lipoprotein (LDL), and high-density lipoprotein (HDL) levels in patients with AMI were detected using enzyme-linked immunosorbent assay (ELISA) at ZT4 and ZT16. NS, not significance, $^{*}P < 0.05$, $^{**}P < 0.005$, $^{***}P < 0.0005$, $^{****}P < 0.0001$.

plaque stability, we tested whether targeted inhibition of AK023617 can prevent diurnal variations of atherosclerotic lesions. We verified the reductions in AK023617 expression in the aortas of mice injected with AAV2/9 vectors carrying sh-AK023617 compared with those of mice injected with saline and mice injected with vectors carrying sh-NC at ZT16, which was the time of the expression peak of AK023617 (Fig. S4). According to histopathological examination, inhibition of AK023617 protected mice from AS at ZT16 because of the lower proportion of the necrotic core, higher collagen fibrous caps, and decreased cholesterol crystals in sh-AK023617-injected mice than in saline-injected mice and sh-NC-injected mice (Fig. 3A–F). In addition, the expression of P-RIP3/RIP3 and P-MLKL/MLKL-related to necroptosis in the aortas at ZT16 was notably reduced (Fig. 3G–I). These results indicate that inhibition of AK023617 disturbs diurnal variations of necroptosis in atherosclerotic lesions *in vivo*.

3.4. Oscillating lncRNA-AK023617 promotes the rhythmic expression of IRGM

To further explore the mechanism by which diurnally expressed AK023617 participates in circadian regulation of necroptosis in plaques, we constructed a lncRNA-mRNA interaction network centered on AK023617 (GSE157878). The result showed that murine AK023617 had the largest correlation coefficient with Irgm1 expression (Fig. 4A). To explore the relationship between IRGM and diurnal occurrence of acute adverse events, we measured IRGM levels in the peripheral blood of patients with AMI. Fig. 4B shows that IRGM expression was rhythmical, with a peak at ZT16 and trough at ZT4, which were consistent with AK023617. Unexpectedly, the expression of AK023617 and IRGM did not exhibit significant rhythmic characteristics in physiological states. Circadian rhythm parameters of AK023617 and IRGM were not observed in synchronized THP-1s, but similar circadian expression patterns were observed in serum-shocked THP-1s stimulated with ox-LDL (Fig. 4C–G). The expression of AK023617 was positively correlated with IRGM mRNA expression in synchronized THP-1s stimulated with ox-LDL (Fig. 4H). However, knockdown of AK023617 in THP-1 cells disrupted the circadian expression of IRGM; the expression of IRGM did not differ between ZT0 and ZT12 (Fig. S5 and Fig. 4I–L). These results show that the ablation of AK023617 under pathological conditions of inflammatory stimulation led to a decrease in IRGM expression and disrupted the rhythmicity.

3.5. LncRNA-AK023617 increases macrophage necroptosis via IRGM

To verify the role of AK023617 in macrophage necroptosis, as shown in Fig. 5A and B, we performed flow cytometry analysis, which revealed

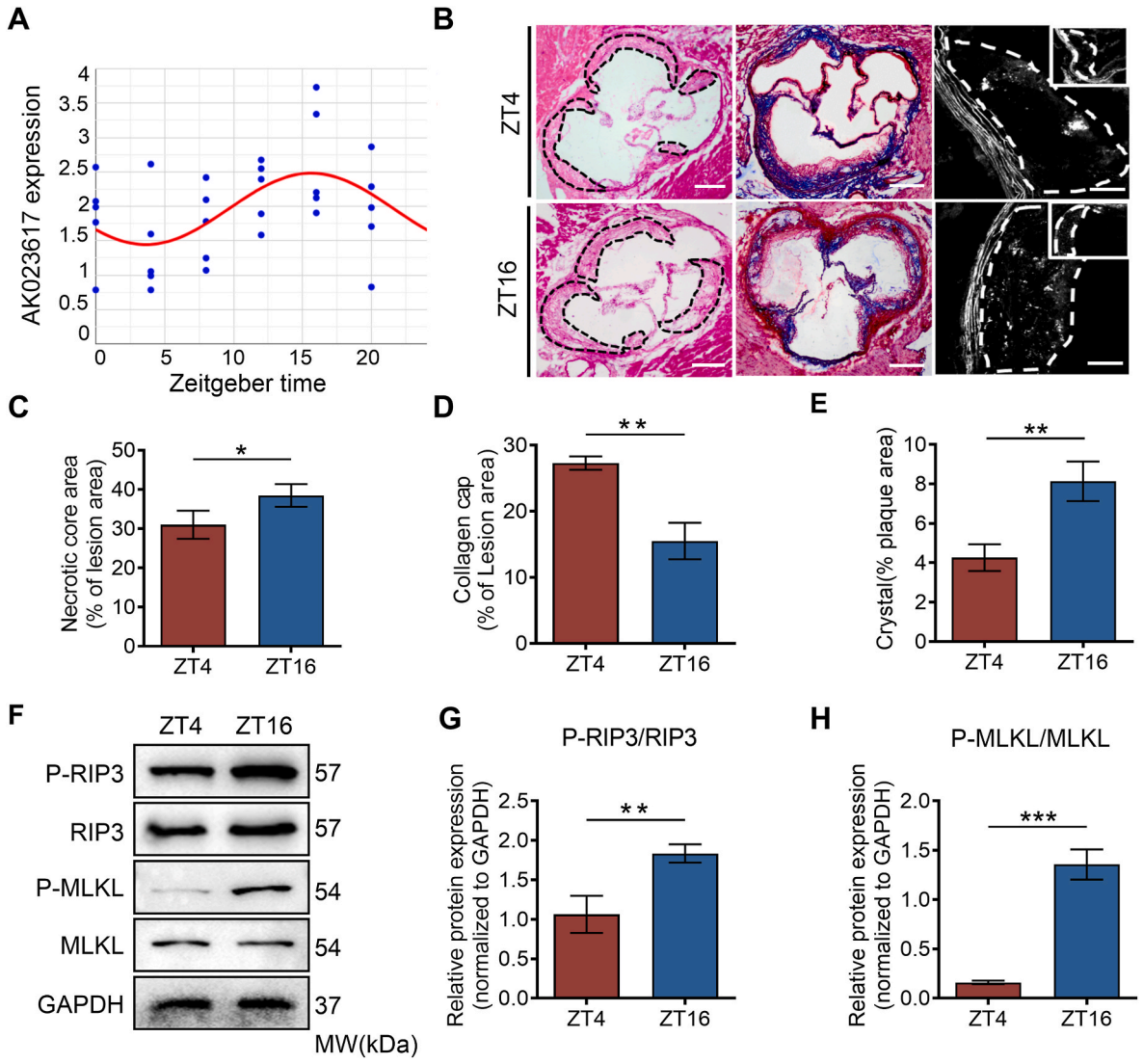

Fig. 2. LncRNA-AK023617 was rhythmically expressed in atherosclerotic lesions with a pattern similar to the indicators of necroptosis. A Aortas of ApoE$^{-/-}$ mice fed a high-fat diet for 12 weeks were harvested at 4 h intervals and murine lncAK023617 expression was measured using RT-qPCR. The rhythmicity of murine lncAK023617 was analyzed; median = 1.96285, amplitude = 0.51867848, peak = 15.63767801, $P < 0.05$, n = 3. **B** Representative images of hematoxylin and eosin staining to assess the necrotic lipid core, collagen in the aortic sinus detected by Masson trichrome staining, and cholesterol crystals imaged by confocal microscopy in aortic root sections from ApoE$^{-/-}$ mice at ZT4 and ZT16, necrotic lipid core, collagen, bar = 200 μm; cholesterol crystals, bar = 50 μm. **C** Percentage of necrotic core areas in the plaques. **D** Quantitative analyses of the percentage of collagen content in the plaques. **E** Quantitative analysis of the percentage of cholesterol crystals in the plaques. **F–H** Representative blots and quantification of RIP3/MLKL pathway-induced necroptosis in aortas of ApoE$^{-/-}$ mice, n = 3. *$P < 0.05$, **$P < 0.005$, ***$P < 0.0005$, ****$P < 0.0001$.

that late apoptosis or necroptosis (upper right quadrants) was reduced in THP-1 cells with siRNA-induced low AK023617 or IRGM expression than that in cells stimulated with ox-LDL alone. In addition, the classical necroptosis-related proteins phosphorylated RIP3 and phosphorylated MLKL were reduced in THP-1 cells transfected with si-AK023617 or si-IRGM, whereas RIP3 or MLKL were unchanged (Fig. 5C–E). A more pronounced reduced necroptosis was detected in cells in which both AK023617 and IRGM were knocked down in combination with ox-LDL exposure (Fig. 5). These results demonstrate that knockdown of AK023617 and IRGM significantly inhibits macrophage necroptosis *in vitro*.

3.6. *LncRNA-AK023617 promotes nuclear translocation of Bmal1 to maintain circadian regulation of IRGM*

We next explored the molecular mechanism by which AK023617 regulates rhythmic expression of IRGM. AK023617 was primarily localized in the cytoplasm of THP-1 cells (Fig. 6A). LncRNA–protein interactions can affect protein stability, activity, and localization [26]. RNA pull-down assays followed by silver staining and RNA immunoprecipitation identified Bmal1 (~78 kDa) as a cytoplasmic protein interacting with AK023617 (Fig. 6B–D and Table S3). The BMAL1/CLOCK complex enters the nucleus through BMAL1-dependent shuttling, and shuttling of BMAL1 dynamically controls transcription activation activity and proteolysis of BMAL1/CLOCK heterodimers. Our results showed that AK023617 knockdown inhibited the translocation of Bmal1 from the cytoplasm to the nucleus (Fig. 6E–G). The JASPAR database predicted that Bmal1 could bind to an E-box sequence in the IRGM promoter (Fig. 6H). We also analyzed a previously published GEO dataset (GSE95712) [27] and found a significant peak of BMAL1 binding to the IRGM promoter (Fig. 6I). ChIP assays confirmed that Bmal1 was recruited to the promoter of IRGM in synchronized THP-1 cells stimulated with ox-LDL in a circadian time-dependent manner (Fig. 6J). Notably, Bmal1 recruitment was more extensive at ZT0 than at ZT12

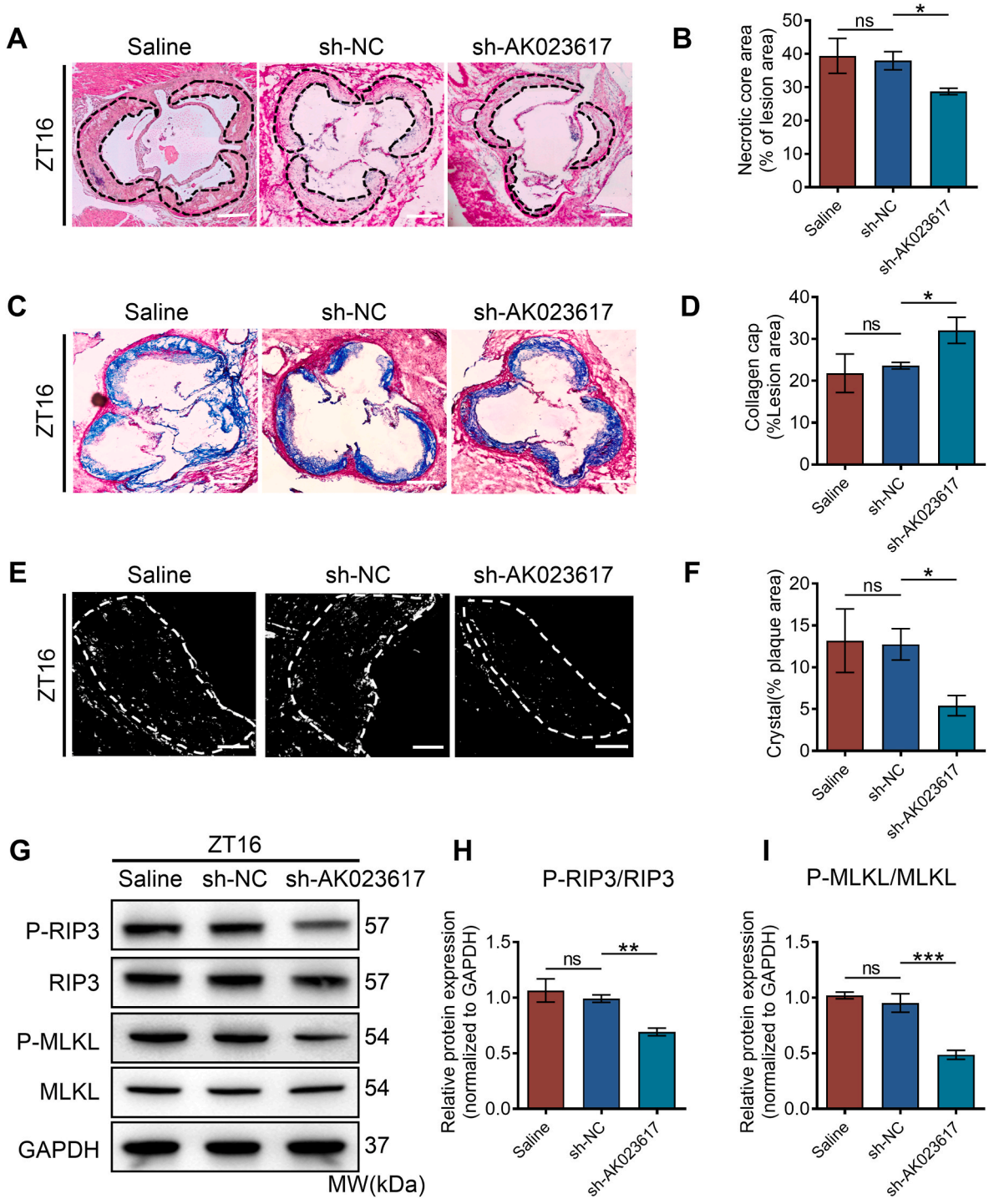

Fig. 3. Inhibition of lncRNA-AK023617 decreased progression of atherosclerosis at ZT16 in ApoE$^{-/-}$ mice *in vivo*
After HFD feeding for 12 weeks, ApoE$^{-/-}$ mice received a single injection of saline or AAV2/9 vectors carrying negative control shRNA (sh-NC) or AK023617 (sh-AK023617) through their tail veins at ZT16. On day 15, the aortas and hearts were harvested. **A–B** Representative images and quantitative analysis using hematoxylin and eosin staining in aortic root sections to assess the necrotic lipid core; bar = 200 μm. **C–D** Collagen in the aortic sinus detected by Masson trichrome staining and quantitative analyses of the percentage of collagen content in the plaques, bar = 200 μm. **E–F** Cholesterol crystals were imaged by confocal microscopy and quantitatively analyzed to determine the percentage of cholesterol crystals in the plaques; bar = 50 μm. **G–I** Representative blots and quantification of RIP3/MLKL pathway-induced necroptosis in aortas from sh-AK023617-injected mice, saline-injected mice and sh-NC-injected mice, n = 3. NS, not significant, $^{*}P < 0.05$, $^{**}P < 0.005$, $^{***}P < 0.0005$, $^{****}P < 0.0001$.

(Fig. 6J). Based on these results, AK023617 may affect nuclear translocation of BMAL1/CLOCK to regulate the rhythmic expression of IRGM.

4. Discussion

Circadian rhythms are involved in physiology and the development of cardiovascular disease. The timing of treatment administration for cardiovascular diseases can have a crucial effect on efficacy and the

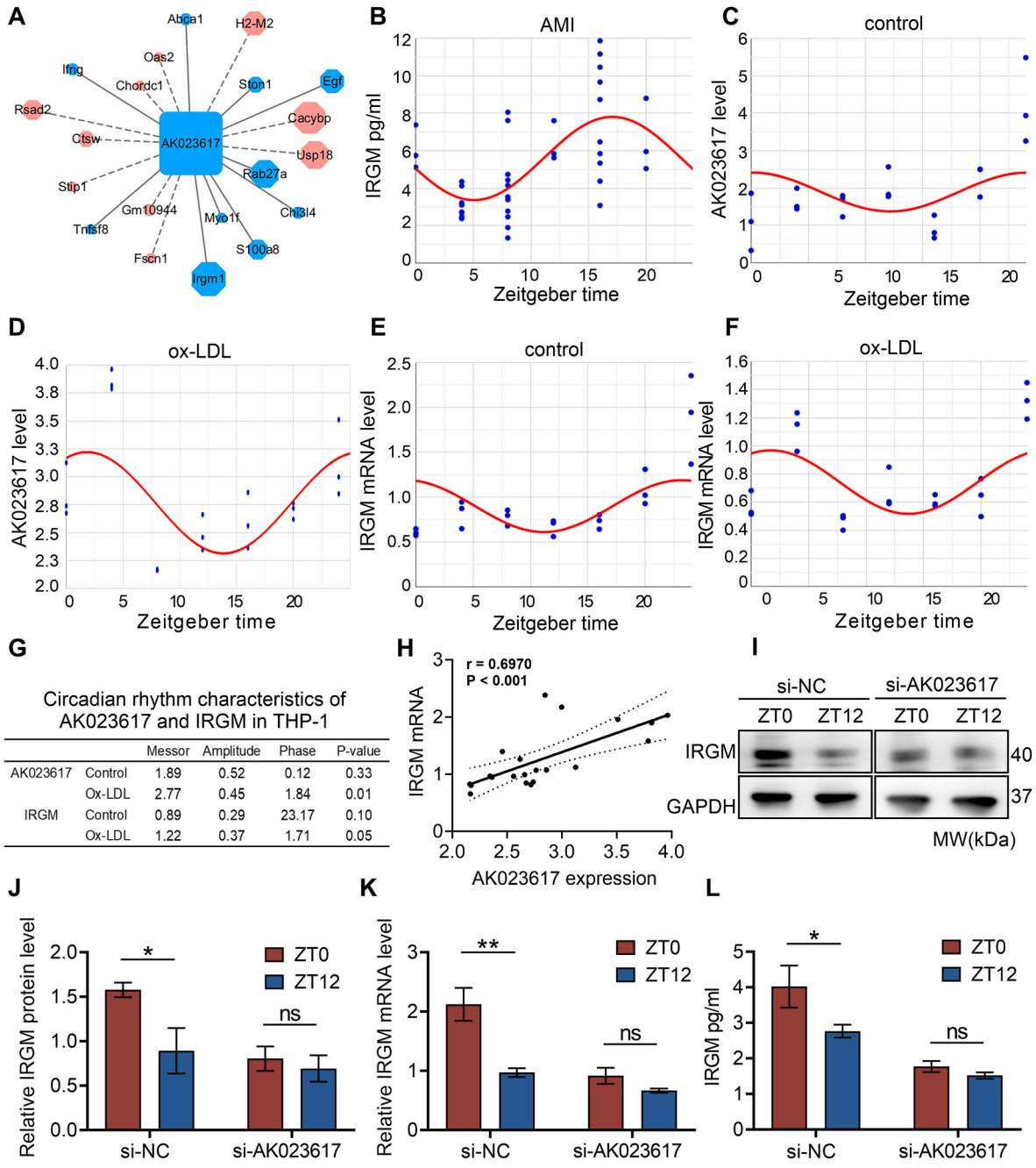

		Messor	Amplitude	Phase	P-value
AK023617	Control	1.89	0.52	0.12	0.33
	Ox-LDL	2.77	0.45	1.84	0.01
IRGM	Control	0.89	0.29	23.17	0.10
	Ox-LDL	1.22	0.37	1.71	0.05

Fig. 4. Oscillating lncRNA-AK023617 promotes rhythmic expression of IRGM. A AK023617-related coding gene network diagram. **B** IRGM levels in peripheral blood of patients with AMI were measured using ELISA. The rhythmicity of IRGM was analyzed; mesor = 5.57952, amplitude = 2.220842, acrophase = 17.078, $P < 0.05$, n = 56. **C–D** Circadian expression of AK023617 was determined in synchronized THP-1 cells stimulated with or without ox-LDL (50 μg/mL) by RT-qPCR. **E–F** Circadian rhythm of IRGM was determined in synchronized THP-1 cells stimulated with or without ox-LDL (50 μg/mL) by RT-qPCR. **G** Circadian rhythm characteristics of AK023617 and IRGM. **H** Correlation of AK023617 and IRGM by Pearson correlation test. **I–J** Representative blots and quantification of IRGM at ZT0 and ZT12 in THP-1s after transfection with si-NC or si-lncAK023617. **K–L** IRGM levels were measured using ELISA and RT-qPCR at ZT0 and ZT12 in THP-1 cells after transfection with si-NC or si-lncAK023617. NS, not significant, $^{*}P < 0.05$, $^{**}P < 0.005$, $^{***}P < 0.0005$, $^{****}P < 0.0001$.

occurrence of adverse effects [28]. Many of these diseases exhibit a 24-h rhythm in incidence; traditionally, these circadian variations were ascribed to sympathetic activity, shear stress, and cardiovascular risk factors such as blood pressure [29]. In this study, we first identified an oscillating lncRNA-AK023617 in macrophages and examined the underlying mechanisms linking circadian rhythm and AS. We confirmed that AK023617 controlled diurnal rhythm in IRGM expression by altering the nuclear translocation of Bmal1, thereby regulating necroptosis of macrophages and decreasing plaque stability.

Clinical data and animal studies confirmed that plaque stability exhibits a diurnal variation pattern. Systematic studies of the onset time of AMI in different regions of the world (including Asia [30], Europe [31], and the USA [32]) showed that there is a diurnal rhythm in the occurrence of AMI but the peak can differ according to the geographical location and climatic conditions. Here, we found that the peak of AMI occurrence in Heilongjiang province, China is 21:00–1:00, which is slightly different from epidemiological data. This may be because of the geographical location of Heilongjiang, which is in a high-latitude region. Atherosclerotic plaque rupture causes up to 75 % of acute coronary syndrome episodes [10], suggesting that diurnal oscillations in plaque

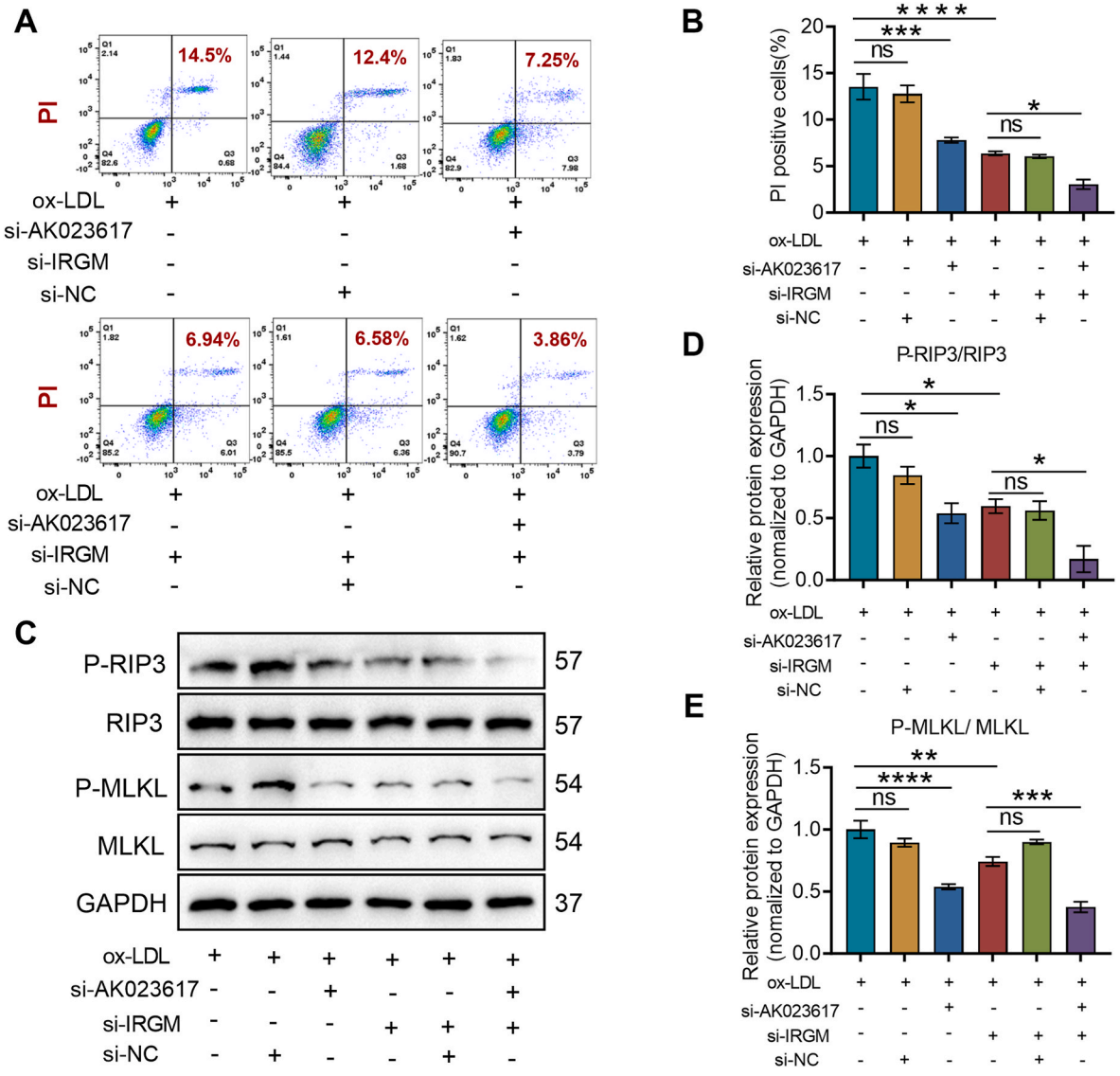

Fig. 5. LncRNA-AK023617 increases necroptosis via IRGM in THP-1 cells. A–B Necroptosis levels in THP-1 cells (propidium iodide-positive cells) detected using flow cytometry. **C–E** Representative blots and quantification of RIP3/MLKL pathway-induced necroptosis in THP-1 cells. NS, not significant, $^{*}P < 0.05$, $^{**}P < 0.005$, $^{***}P < 0.0005$, $^{****}P < 0.0001$.

stability are associated with the incidence of acute adverse events. In clinical studies, the maximum lipid arc had a diurnal variation; however, the mini fibrous cap thickness and minimal lumen area showed no significant changes throughout the day. These results suggest that the circadian rhythm plays a role in plaque stability but does not significantly alter the existing plaque morphology. Additionally, our results showed that clinical manifestations of patients with AMI coincide with circadian oscillations of circulating parameters, including lipid risk factors such as LDL, triglycerides, and total cholesterol. In line with the clinical phenomena, animal studies showed revealed a circadian expression pattern in the indicators of plaque stability in aortic root lesions, such as the percentage of necrotic core, collagen cap, and crystals (Fig. 2B–E). These results suggest that diurnal oscillations exist in plaque stability, which may be associated with the incidence of acute adverse events.

Circulating lncRNAs are biomarkers in AS and other cardiovascular diseases, but their functions in cardiac biology and disease are largely unclear, particularly those of oscillating lncRNA [33]. In blood of patients with AMI, we found a significant oscillating lncRNA-AK023617 (Fig. 1C). The peak and trough expression of murine AK023617 in atherosclerotic arteries was consistent with indicators of plaque stability (Fig. 2A–E). The expression of RIPK3 and MLKL is elevated in human atherosclerotic plaques [15]. Atherosclerotic mice exhibited a comparable circadian rhythm in the phosphorylation of RIPK3 and MLKL within aortic root lesions when AK023617 was expressed. In contrast, the diminished expression of AK023617 *in vivo* disrupted the diurnal variations of necroptosis in atherosclerotic lesions. This result suggests that the diurnal rhythms of AK023617 control the daily oscillations in necroptosis. RIPK1 colocalizes mainly with macrophages, supporting that macrophage are involved in necroptosis in AS [34]. Furthermore, the level of representative markers of necroptosis in THP-1-derived foam cells was significantly increased after serum starvation [35]. More importantly, Fig. 4 shows that IRGM was a downstream mediator of AK023617 in synchronized THP-1 cells and stimulated with ox-LDL after serum starvation. Our previous study revealed that IRGM promotes macrophage apoptosis in plaques, thus aggravating AS progression [23]. We identified the pathological rhythmicity of IRGM, and the peak was consistent with the incidence of acute adverse events in patients with AMI. Swati Roy confirmed that IRGM regulates necroptosis and the release of damage-associated molecular patterns to induce

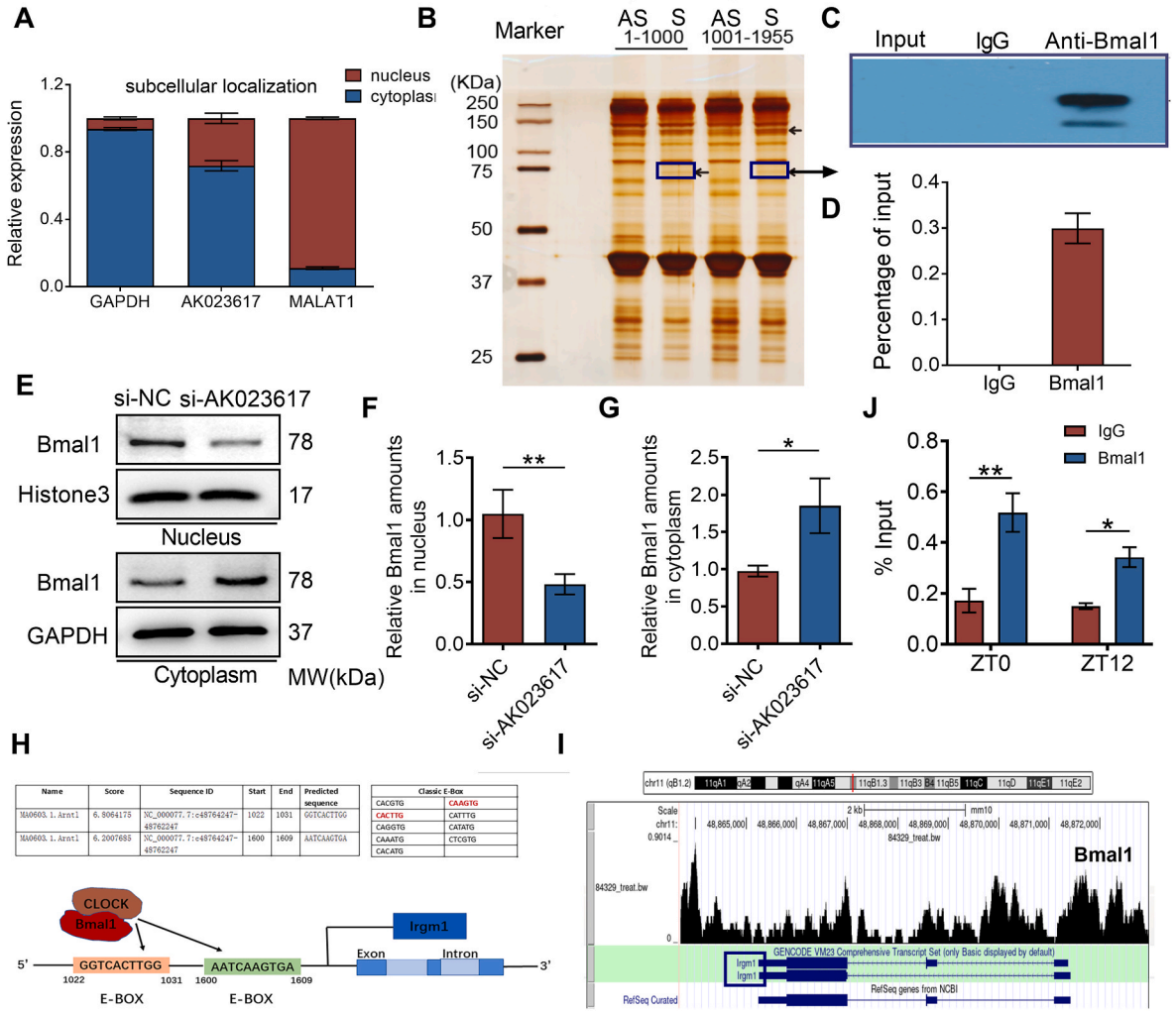

Fig. 6. LncRNA-AK023617 interacts with Bmal1 to regulate circadian expression of IRGM. A Cytoplasmic and nuclear levels of lncRNA-AK023617 in THP-1 cells. **B** Silver staining of protein mixtures following an RNA pull-down assay in THP-1 cells. **C** Western blotting analysis of the interaction of Bmal1 with AK023617 probe following RNA pull-down assay. **D** RNA immunoprecipitation assay showing an interaction between Bmal1 and AK023617. **E–G** Representative blots and quantification of cytoplasmic and nuclear Bmal1 levels in THP-1 cells transfected with scrambled siRNA or siRNA targeting lncAK023617 and treated with oxidized low-density lipoprotein (ox-LDL; 50 μg/mL). **H** Potential binding sites for the Bmal1/Clock heterodimer in the *IRGM* promoter were analyzed using the JASPAR database. **I** Fastq data for ChIP-seq samples from Gene Expression Omnibus (GEO) series GSE95712 were analyzed using Genome-wide Event finding and Motif discovery (GEM) and visualized with the UCSC genome browser. **J** ChIP assays showing recruitment of Bmal1 protein to the promoter of IRGM in synchronized THP-1 cells stimulated with ox-LDL (50 μg/mL) at ZT0 and ZT12, n = 3. NS, not significant, $^{*}P < 0.05$, $^{**}P < 0.005$, $^{***}P < 0.0005$, $^{****}P < 0.0001$.

gastrointestinal inflammation in Crohn's disease [36]. As expected, we found that AK023617 induced macrophage necroptosis via IRGM.

The Bmal1/Clock heterodimer functions as a transcription factor that regulates the rhythmic expression of mammalian genes. We confirmed that AK023617 is highly expressed in the cytoplasm of THP-1 cells and RNA pull-down and RIP collectively showed that it binds to Bmal1. As core clock gene, the protein stability and nucleoplasmic distribution of Bmal1 can affect its function in regulating circadian oscillation [37]. Our results in Fig. 6 show that knockdown of AK023617 in THP-1 cells reduced Bmal1 protein levels in nuclear fractions, suggesting that AK023617 controls circadian oscillation of IRGM by regulating intracellular shuttling of Bmal1.

Targeting the time has applied in cardiovascular diseases. An important treatment strategy is to decrease cardiovascular risk factors at the time of day when they are highest [38]. Targeting AK023617 at a specific time of day may be benefit patients with AMI. We also explored a pharmacological intervention that targets necroptosis by stabilizing vulnerable plaques and improving the effectiveness of anti-atherosclerotic therapies. Human blood metabolites, such as glucose, low-density lipoprotein, triglycerides, and the regulating hormone insulin oscillate throughout the day [39]. Our results showed the expression of AK023617 in the blood of patients with AMI coincides with circadian oscillations of lipid risk factors. The involvement of AK023617 in these oscillations requires further examination. In addition, in advanced plaques, foam cells undergo diverse pathways of programmed cell death, including apoptosis, necroptosis, pyroptosis, and autosis, contributing to the necrotic cores of atherosclerotic plaques [40]. Thus, the risk that inhibiting one form of cell death can result in activation of another form of cell death should be considered [14].

In summary, we identified the oscillating lncRNA-AK021617, whose expression pattern is closely related to plaque stability in patients with AMI and atherosclerotic mice. Mechanistically, circadian expression of lncRNA AK023617 in macrophages regulates diurnal oscillations in necroptosis by modulating the diurnal rhythm of IRGM, providing a macrophage death clock that contributes to atherosclerotic plaque instability. AK023617 is an attractive RNA therapeutic target to ameliorate the incidence of major adverse cardiovascular events.

CRediT authorship contribution statement

Rongzhe Lu: Writing – original draft, Visualization, Validation, Software, Investigation, Formal analysis, Data curation. **Hengxuan Cai:** Writing – original draft, Software, Project administration, Funding acquisition. **Yige Liu:** Validation, Investigation, Data curation. **Guanpeng Ma:** Visualization, Validation, Software. **Jiaxin Wang:** Visualization, Validation, Methodology. **Miao Yan:** Software, Methodology, Investigation. **Zhenming Zhang:** Visualization, Software, Investigation. **Bo Yu:** Writing – review & editing, Funding acquisition, Conceptualization. **Zhaoying Li:** Writing – review & editing, Data curation, Conceptualization. **Shaohong Fang:** Writing – review & editing, Funding acquisition, Conceptualization.

Data availability

The datasets used and analyzed during the current study are available from the corresponding author on reasonable request.

Ethics approval statement

This study complies with the basic principles of the *Declaration of Helsinki* and was approved by the Ethics Committee of the 2nd Affiliated Hospital of Harbin Medical University (Harbin, China), Ethics No. KY2018-082. All patients provided written informed consent. All interventions and animal care methods were conducted according to the Guide for the Care and Use of Laboratory Animals by the US National Institutes of Health (NIH Publication No. 85–23, revised in 2011) and the Animal Ethics Committee of the Second Affiliated Hospital of Harbin Medical University (Harbin, China), Ethics No. Sydwgzr2021-096.

Funding

This work was funded by the National Natural Science Foundation of China (82170262,82370265, 82200546, 62135002), The Second Affiliated Hospital of Harbin Medical University Foundation (PYQN2023-10), Key Laboratory of Myocardial Ischemia, Ministry of Education (KF202213), Heilongjiang Provincial Key Research & Development Program (2023ZX02C11).

Declaration of competing interest

The authors declare that they have no known competing financial interests or personal relationships that could have appeared to influence the work reported in this paper.

Appendix A. Supplementary data

Supplementary data to this article can be found online at https://doi.org/10.1016/j.ncrna.2024.12.008.

Supplementary information is available at Non-coding RNA Research's website.

Online Figures S1-S5.

References

[1] J.J. Gooley, J. Lu, T.C. Chou, T.E. Scammell, C.B. Saper, Melanopsin in cells of origin of the retinohypothalamic tract, Nat. Neurosci. 4 (2001) 1165, https://doi.org/10.1038/nn768.
[2] D.P. King, J.S. Takahashi, Molecular genetics of circadian rhythms in mammals, Annu. Rev. Neurosci. 23 (2000) 713–742, https://doi.org/10.1146/annurev.neuro.23.1.713.
[3] J.O. Early, A.M. Curtis, Immunometabolism: is it under the eye of the clock? Semin. Immunol. 28 (2016) 478–490, https://doi.org/10.1016/j.smim.2016.10.006.
[4] W.J. Elliott, Circadian variation in the timing of stroke onset: a meta-analysis, Stroke 29 (1998) 992–996, https://doi.org/10.1161/01.str.29.5.992.
[5] J.E. Muller, P.H. Stone, Z.G. Turi, J.D. Rutherford, C.A. Czeisler, C. Parker, et al., Circadian variation in the frequency of onset of acute myocardial infarction, N. Engl. J. Med. 313 (1985) 1315–1322, https://doi.org/10.1056/nejm198511213132103.
[6] N. Twidale, S. Taylor, W.F. Heddle, B.F. Ayres, A.M. Tonkin, Morning increase in the time of onset of sustained ventricular tachycardia, Am. J. Cardiol. 64 (1989) 1204–1206, https://doi.org/10.1016/0002-9149(89)90881-3.
[7] S.N. Willich, R.J. Goldberg, M. Maclure, L. Perriello, J.E. Muller, Increased onset of sudden cardiac death in the first three hours after awakening, Am. J. Cardiol. 70 (1992) 65–68, https://doi.org/10.1016/0002-9149(92)91391-g.
[8] P. Hou, J. Fang, Z. Liu, Y. Shi, M. Agostini, F. Bernassola, et al., Macrophage polarization and metabolism in atherosclerosis, Cell Death Dis. 14 (2023) 691, https://doi.org/10.1038/s41419-023-06206-z.
[9] A.W.C. Man, H. Li, N. Xia, Circadian rhythm: potential therapeutic target for atherosclerosis and thrombosis, Int. J. Mol. Sci. 22 (2021), https://doi.org/10.3390/ijms22020676.
[10] J. Narula, M. Nakano, R. Virmani, F.D. Kolodgie, R. Petersen, R. Newcomb, et al., Histopathologic characteristics of atherosclerotic coronary disease and implications of the findings for the invasive and noninvasive detection of vulnerable plaques, J. Am. Coll. Cardiol. 61 (2013) 1041–1051, https://doi.org/10.1016/j.jacc.2012.10.054.
[11] M.M. Kavurma, K.J. Rayner, D. Karunakaran, The walking dead: macrophage inflammation and death in atherosclerosis, Curr. Opin. Lipidol. 28 (2017) 91–98, https://doi.org/10.1097/mol.0000000000000394.
[12] G. Kung, K. Konstantinidis, R.N. Kitsis, Programmed necrosis, not apoptosis, in the heart, Circ. Res. 108 (2011) 1017–1036, https://doi.org/10.1161/circresaha.110.225730.
[13] T. Vanden Berghe, A. Linkermann, S. Jouan-Lanhouet, H. Walczak, P. Vandenabeele, Regulated necrosis: the expanding network of non-apoptotic cell death pathways, Nat. Rev. Mol. Cell Biol. 15 (2014) 135–147, https://doi.org/10.1038/nrm3737.
[14] G.R.Y. De Meyer, M. Zurek, P. Puylaert, W. Martinet, Programmed death of macrophages in atherosclerosis: mechanisms and therapeutic targets, Nat. Rev. Cardiol. 21 (2024) 312–325, https://doi.org/10.1038/s41569-023-00957-0.
[15] D. Karunakaran, M. Geoffrion, L. Wei, W. Gan, L. Richards, P. Shangari, et al., Targeting macrophage necroptosis for therapeutic and diagnostic interventions in atherosclerosis, Sci. Adv. 2 (2016) e1600224, https://doi.org/10.1126/sciadv.1600224.
[16] X. Zhang, Z. Ren, W. Xu, Z. Jiang, Necroptosis in atherosclerosis, Clin. Chim. Acta 534 (2022) 22–28, https://doi.org/10.1016/j.cca.2022.07.004.
[17] A. Schober, R.M. Blay, S. Saboor Maleki, F. Zahedi, A.E. Winklmaier, M.Y. Kakar, et al., MicroRNA-21 controls circadian regulation of apoptosis in atherosclerotic lesions, Circulation 144 (2021) 1059–1073, https://doi.org/10.1161/circulationaha.120.051614.
[18] Z. Li, P. Gong, W. Wang, S. Qu, X. Wang, Z. He, et al., Functional network analysis reveals biological roles of lncRNAs and mRNAs in MOG(35-55) specific CD4(+)T helper cells, Genomics 110 (2018) 337–346, https://doi.org/10.1016/j.ygeno.2018.01.012.
[19] M. Yang, M. Zhang, Z. Li, J. Liu, Y. Li, Z. Yang, et al., A landscape of Long non-coding RNAs reveals the leading transcriptome alterations in murine aorta during aging, Genomics 115 (2023) 110573, https://doi.org/10.1016/j.ygeno.2023.110573.
[20] R. Brooks, J. Monzy, B. Aaron, X. Zhang, A. Kossenkov, J. Hayden, et al., Circadian lncRNA ADIRF-AS1 binds PBAF and regulates renal clear cell tumorigenesis, Cell Rep. 41 (2022) 111514, https://doi.org/10.1016/j.celrep.2022.111514.
[21] Y. Lin, S. Wang, L. Gao, Z. Zhou, Z. Yang, J. Lin, et al., Oscillating lncRNA Platr4 regulates NLRP3 inflammasome to ameliorate nonalcoholic steatohepatitis in mice, Theranostics 11 (2021) 426–444, https://doi.org/10.7150/thno.50281.
[22] X. Wu, L. Chen, F. Zeb, Y. Huang, J. An, J. Ren, et al., Regulation of circadian rhythms by NEAT1 mediated TMAO-induced endothelial proliferation: a protective role of asparagus extract, Exp. Cell Res. 382 (2019) 111451, https://doi.org/10.1016/j.yexcr.2019.05.032.
[23] S. Fang, S. Sun, H. Cai, X. Zou, S. Wang, X. Hao, et al., IRGM/Irgm1 facilitates macrophage apoptosis through ROS generation and MAPK signal transduction: Irgm1(+/-) mice display increases atherosclerotic plaque stability, Theranostics 11 (2021) 9358–9375, https://doi.org/10.7150/thno.62797.
[24] H. Itaya, T. Takagi, K. Sugi, M. Nakamura, Contents of second peak in the circadian variation of acute myocardial infarction in the Japanese population, J. Cardiol. 59 (2012) 147–153, https://doi.org/10.1016/j.jjcc.2011.11.011.
[25] S. Jiang, C. Fang, X. Xu, L. Xing, S. Sun, C. Peng, et al., Identification of high-risk coronary lesions by 3-vessel optical coherence tomography, J. Am. Coll. Cardiol. 81 (2023) 1217–1230, https://doi.org/10.1016/j.jacc.2023.01.030.
[26] M. Guttman, J.L. Rinn, Modular regulatory principles of large non-coding RNAs, Nature 482 (2012) 339–346, https://doi.org/10.1038/nature10887.
[27] Y. Oishi, S. Hayashi, T. Isagawa, M. Oshima, A. Iwama, S. Shimba, et al., Bmal1 regulates inflammatory responses in macrophages by modulating enhancer RNA transcription, Sci. Rep. 7 (2017) 7086, https://doi.org/10.1038/s41598-017-07100-3.
[28] N. Takeda, K. Maemura, S. Horie, K. Oishi, Y. Imai, T. Harada, et al., Thrombomodulin is a clock-controlled gene in vascular endothelial cells, J. Biol. Chem. 282 (2007) 32561–32567, https://doi.org/10.1074/jbc.M705692200.
[29] R. Manfredini, M. Gallerani, F. Portaluppi, C. Fersini, Relationships of the circadian rhythms of thrombotic, ischemic, hemorrhagic, and arrhythmic events to blood pressure rhythms, Ann. N. Y. Acad. Sci. 783 (1996) 141–158, https://doi.org/10.1111/j.1749-6632.1996.tb26713.x.
[30] Y. Li, T. Du, M.R. Lewin, H. Wang, X. Ji, Y. Zhang, et al., Circadian, day-of-week, and age patterns of the occurrence of acute coronary syndrome in Beijing's

emergency medical services system, Am. J. Emerg. Med. 28 (2010) 663–667, https://doi.org/10.1016/j.ajem.2009.02.033.
[31] C. Savopoulos, A. Ziakas, A. Hatzitolios, C. Delivoria, A. Kounanis, S. Mylonas, et al., Circadian rhythm in sudden cardiac death: a retrospective study of 2,665 cases, Angiology 57 (2006) 197–204, https://doi.org/10.1177/000331970605700210.
[32] R.J. Goldberg, P. Brady, J.E. Muller, Z.Y. Chen, M. de Groot, P. Zonneveld, et al., Time of onset of symptoms of acute myocardial infarction, Am. J. Cardiol. 66 (1990) 140–144, https://doi.org/10.1016/0002-9149(90)90577-n.
[33] M. Cao, H. Luo, D. Li, S. Wang, L. Xuan, L. Sun, Research advances on circulating long noncoding RNAs as biomarkers of cardiovascular diseases, Int. J. Cardiol. 353 (2022) 109–117, https://doi.org/10.1016/j.ijcard.2022.01.070.
[34] I. Coornaert, P. Puylaert, G. Marcasolli, M.O.J. Grootaert, P. Vandenabeele, G.R. Y. De Meyer, et al., Impact of myeloid RIPK1 gene deletion on atherogenesis in ApoE-deficient mice, Atherosclerosis 322 (2021) 51–60, https://doi.org/10.1016/j.atherosclerosis.2021.02.021.
[35] F. Tian, J. Yao, M. Yan, X. Sun, W. Wang, W. Gao, et al., 5-Aminolevulinic acid-mediated sonodynamic therapy inhibits RIPK1/RIPK3-dependent necroptosis in THP-1-derived foam cells, Sci. Rep. 6 (2016) 21992, https://doi.org/10.1038/srep21992.
[36] S. Roy, A. Esmaeilniakooshkghazi, S. Patnaik, Y. Wang, S.P. George, A. Ahrorov, et al., Villin-1 and gelsolin regulate changes in actin dynamics that affect cell survival signaling pathways and intestinal inflammation, Gastroenterology 154 (2018) 1405–1420, https://doi.org/10.1053/j.gastro.2017.12.016.
[37] I. Kwon, J. Lee, S.H. Chang, N.C. Jung, B.J. Lee, G.H. Son, et al., BMAL1 shuttling controls transactivation and degradation of the CLOCK/BMAL1 heterodimer, Mol. Cell Biol. 26 (2006) 7318–7330, https://doi.org/10.1128/mcb.00337-06.
[38] A. De Giorgi, A. Mallozzi Menegatti, F. Fabbian, F. Portaluppi, R. Manfredini, Circadian rhythms and medical diseases: does it matter when drugs are taken? Eur. J. Intern. Med. 24 (2013) 698–706, https://doi.org/10.1016/j.ejim.2013.03.019.
[39] S. Steffens, C. Winter, M.J. Schloss, A. Hidalgo, C. Weber, O. Soehnlein, Circadian control of inflammatory processes in atherosclerosis and its complications, Arterioscler. Thromb. Vasc. Biol. 37 (2017) 1022–1028, https://doi.org/10.1161/atvbaha.117.309374.
[40] Y. Gui, H. Zheng, R.Y. Cao, Foam cells in atherosclerosis: novel insights into its origins, consequences, and molecular mechanisms, Front Cardiovasc Med 9 (2022) 845942, https://doi.org/10.3389/fcvm.2022.845942.